International Journal of Nanomedicine

Dovepress
open access to scientific and medical research

Open Access Full Text Article

ORIGINAL RESEARCH

Suppression of lung cancer progression by biocompatible glycerol triacrylate–spermine-mediated delivery of shAkt1

This article was published in the following Dove Press journal:
International Journal of Nanomedicine
3 May 2012
Number of times this article has been viewed

Seong-Ho Hong[1,*]
Ji-Eun Kim[1,6,*]
You-Kyoung Kim[2]
Arash Minai-Tehrani[1]
Ji-Young Shin[1]
Bitna Kang[1]
Hye-Joon Kim[1]
Chong-Su Cho[2]
Chanhee Chae[3]
Hu-Lin Jiang[1]
Myung-Haing Cho[1,4–7]

[1]Laboratory of Toxicology, [2]Department of Agricultural Biotechnology and Research Institute for Agriculture and Life Sciences, [3]Laboratory of Pathology, College of Veterinary Medicine, [4]Graduate Group of Tumor Biology, [5]Center for Food and Toxicology, Seoul National University, Seoul, Korea; [6]Department of Nano Fusion Technology, Graduate School of Convergence Science and Technology, [7]Advanced Institute of Convergence Technology, Seoul National University, Suwon, Korea

*These authors contributed equally to this work

Background: Polyethylenimine (PEI)-based nonviral gene-delivery systems are commonly employed because of their high transfection efficiency. However, the toxic nature of PEI is a significant obstacle in clinical gene therapy. In this study, we developed biocompatible glycerol triacrylate–spermine (GT–SPE) polyspermine as a nanosized gene carrier for potential lung cancer gene therapy.

Methods: The GT–SPE was synthesized using the Michael addition reaction between GT and SPE. The molecular weight was characterized using gel permeability chromatography multiangle laser light scattering and the composition of the polymer was analyzed using proton nuclear magnetic resonance.

Results: The GT–SPE successfully protected the DNA from nucleases. The average particle size of the GT–SPE was 121 nm with a zeta potential of +23.45 mV. The GT–SPE was found to be less toxic than PEI for various cell lines, as well as for a murine model. Finally, our results showed that the GT–SPE/small hairpin Akt1 (shAkt1) complex suppressed lung tumorigenesis in a K-*ras*^{LA1} lung cancer mice model by inducing apoptosis through the Akt signaling pathway and cell cycle arrest. Aerosol delivered GT–SPE/shAkt1, which reduced matrix metalloproteinase-9 activity and suppressed the expression levels of proliferating cell nuclear antigen, as well as vascular endothelial growth factors and CD31, which are known proliferation and angiogenesis markers, respectively.

Conclusion: Our data suggest that GT–SPE may be a candidate for short hairpin-shaped RNA-based aerosol lung cancer gene therapy.

Keywords: lung cancer, gene therapy, aerosol delivery, spermine

RNA interference (RNAi) has attracted significant attention in the research of genetic disorders and infectious diseases, including cancer, because of its therapeutic effects.[1,2] Transfecting synthetic small interfering RNA (siRNA) or plasmid DNA vectors can directly induce RNA interference by expressing short hairpin-shaped RNA (shRNA).[3] Several lines of evidence have demonstrated that shRNA-expressing vectors yielded more durable knockdown effects when compared to siRNA.[4] Naked shRNA has a strong anionic-charged phosphodiester backbone and, as a result, cannot freely cross the cellular membrane. Therefore, viral or nonviral delivery systems that facilitate cellular transfection of shRNA are required.[5] In terms of gene delivery, viral vectors are very efficient, but they have the potential to cause inadequate DNA-carrying capacity, immunogenicity, and mutations in patients.[6,7] In contrast, nonviral vectors are stable, easy to modify, and have been proven to possess high biocompatibility.[8,9] One of the nonviral vectors, polyethylenimine (PEI), is a very effective polymer that can be used

Correspondence: Hu-Lin Jiang
College of Veterinary Medicine,
Seoul National University,
Seoul 151-742, Korea
Tel +82 2 880 1286
Fax +82 2 875 8842
Email jiang3@snu.ac.kr

Myung-Haing Cho
College of Veterinary Medicine,
Seoul National University,
Seoul 151-742, Korea
Tel +82 2 880 1276
Fax +82 2 873 1268
Email mchotox@snu.ac.kr

for gene delivery in any pH condition because of the proton sponge effect.[10] However, PEI is toxic in nature and is also known to stimulate apoptotic pathways.[11,12] As an alternative to nonviral polymer, we have developed polyspermine because of its high transfection efficiency with low in vitro and in vivo toxicity.

We synthesized biocompatible glycerol triacrylate–spermine (GT–SPE) polyspermine using the Michael addition reaction and then validated the complex formation between polymer and DNA. In addition, we analyzed the toxicity and efficiency of transfection both in vitro and in vivo. The GT–SPE was found to be much safer than PEI in both in vitro and in vivo studies. The GT–SPE/DNA also showed high transfection efficiency. Lastly, the antitumor efficacies of GT–SPE/shAkt1 were evaluated using a K-*ras*^{LA1} mouse model of non-small cell lung cancer (NSCLC). The complex exhibited efficient small hairpin Akt1 (shAkt1) delivery and induced apoptosis through the Akt signaling pathway and cell cycle arrest.

Materials and methods

Materials

Glycerol triacrylate (GT) (MW: 254 Da), spermine (MW: 202.34 Da), and anhydrous ethyl alcohol were purchased from Sigma-Aldrich (St Louis, MO). pcDNA3.1/CT-GFP plasmid (6.1 kb) was purchased from Invitrogen (Carlsbad, CA). pcDNA3.1 plasmids were multiplied in *Escherichia coli*, extracted by alkaline lysis, and purified by a QIAGEN kit (QIAGEN, Chatsworth, CA). Luciferase gene, a 5.3 kb pGL3 expression vector that is driven by an SV40 promoter, enhancer, and Cell Titer 96 Aqueous One solution reagent, were purchased from Promega (Madison, WI). Akt1 antibodies were purchased from Cell Signaling (Danvers, MA). Bax, Bcl-xL, proliferating cell nuclear antigen (PCNA), Cyclin B1, vascular endothelial growth factor (VEGF), and Actin antibodies were purchased from Santa Cruz Biotechnology (Santa Cruz, CA). Matrix metalloproteinase-9 (MMP-9) and CD31 antibodies were purchased from Abcam (Cambridge, UK).

Preparation of GT–SPE copolymer

GT–SPE copolymer was synthesized using the Michael addition reaction. GT (1.5 M) and SPE (2.5 M) were separately dissolved in 2 mL of anhydrous ethanol at 4°C, and GT solution was slowly stirred into the SPE solution at 4°C for 2 hours and stored overnight at room temperature. Subsequently, the polymer was dialyzed using Spectra/Por® membrane (MWCO = 3,500) against distilled water at 4°C for 24 hours. Finally, the copolymer was lyophilized and stored at –20°C.

Characterizations of copolymer and GT–SPE/DNA complexes

The composition of the prepared GT–SPE copolymer was estimated by measuring proton nuclear magnetic resonance (^{1}H NMR) using Avance™ 600 spectrometer (Bruker, Karlsruhe, Germany). For measurement of NMR, polymers were dissolved in D_2O at a concentration of 10 mg/mL. The GT–SPE polymer molecular weight was measured by gel permeability chromatography (GPC) with 690 nm laser wavelength (DAWN(R) EOS; Wyatt, Santa Barbara, CA).

All GT–SPE/DNA complexes were freshly prepared before use and characterized using the method described by Jiang et al.[13] Complexes were prepared by adding DNA solution to equal volumes of copolymer solution, vortexing gently, and incubating at room temperature for 30 minutes. The DNA condensation and protection abilities of the GT–SPE polymer were confirmed by electrophoresis. The morphology of GT–SPE/DNA was observed by using an energy-filtering transmission electron microscope (EF-TEM; LIBRA 120; Carl Zeiss, Oberkochen, Germany). The size (scattering angle: 90°) and surface charge (scattering angle: 20°) of the GT–SPE complexes were measured at 25°C using an electrophoretic light-scattering spectrophotometer (ELS 8000; Otsuka Electronics, Osaka, Japan).

Cell viability assay and transfection efficiency studies of GT–SPE

A549 (human lung carcinoma cells; American Type Culture Collection [ATCC], Manassas, VA), HepG2 (human hepatoblastoma cells; ATCC), MCF7 (human breast cancer cells; ATCC), and 16HBE14o- (human bronchial epithelial cells) were cultured in RPMI 1640 (PAA Laboratories, Pashing, Austria), Dulbecco's Modified Eagle Medium (DMEM; PAA Laboratories), and DMEM:Nutrient Mixture F-12 (DMEM/F12; PAA Laboratories), respectively. 16HBE 14o- cells were kindly provided by Dr Dieter C Gruenert (University of California, San Francisco, CA). All of the culture media were supplemented with 10% fetal bovine serum (FBS; PAA Laboratories), streptomycin (100 µg/mL), and penicillin (100 U/mL). All of the cells were incubated at 37°C in a humidified 5% CO_2 atmosphere.

Cell viability and transfection efficiency studies were evaluated according to a method reported previously.[13] For in vitro cytotoxicity tests, cells were seeded in 96-well plates at an initial density of 1×10^4 cells/well in 0.2 mL of growth medium and incubated for 24 hours in advance of the addition of the filtered polymers. Growth media were replaced by serum-free media containing various amounts of polymers.

After additional incubation for 24, 48, and 72 hours, the media were substituted for growth media containing 20 μL of Cell Titer 96® Aqueous One solution reagent. After additional incubation for 3 hours, the absorbance was measured using an ELISA plate reader (GLR 1000; Genelabs Diagnostics, Singapore). For the cell transfection efficiency study, cells were seeded in 24-well plates at an initial density of 1.5×10^5 cells/well in 1 mL of growth medium. After 18 hours of incubation, the media were replaced with serum-free or media with polymer/pGL3 (1 μg) complex and additionally incubated for 4 hours. Subsequently, the media were replaced with fresh media and allowed to incubate for 24 hours at 37°C. The luciferase assay was performed according to the manufacturer's protocol.

In vivo aerosol delivery study

Six-week-old female BALB/c mice (Breeding and Research Center, Seoul National University, Seoul, Korea) were purchased from Joongang Laboratory Animal Inc (Seoul, Korea) and used in accordance with the policy and regulations for the care and use of laboratory animals as provided by Seoul National University, Korea. Animals were kept in the laboratory animal facility with temperature and relative humidity maintained at 23°C ± 2°C and 50% ± 10%, respectively, and with a 12 hour light/dark cycle. Based on previously used methods, mice were placed in a nose-only exposure chamber and exposed to the aerosol for gene delivery.[3] Twelve BALB/c mice were randomly divided into three groups (four mice/group). To check the efficiency of GT–SPE as a gene carrier, treatment groups were exposed to aerosol containing green fluorescent protein (GFP) expression plasmid DNA with and without a carrier, and the remaining group was used as an untreated control. Mice were sacrificed 2 days after exposure and lungs were collected for detection of the GFP signal. Lung tissues were fixed at room temperature and embedded in Tissue-Tek OCT (Sakura, Torrance, CA). Ten micrometers of tissue cryosection were cut with a microtome (Leica, Nussloch, Germany) and mounted on slides for analysis. All the methods used in this study were approved by the Animal Care and Use Committee at Seoul National University (SNU-101211-3).

Six-week-old female K-*ras*^{LA1} mice with human NSCLC were obtained from the Human Cancer Consortium-National Cancer Institute (Frederick, MD) and divided into four groups (four mice/group). Mice were exposed to aerosol using the method described above and the control group mice were left untreated. The other groups were exposed to aerosol containing Akt1 shRNA only or 4 mg GT–SPE and 0.4 mg DNA (scramble or Akt1 shRNA) in distilled water. Treated mice were exposed to aerosol twice a week for 4 consecutive weeks. At the end of the experiment, the mice were sacrificed.[3] During necropsy, neoplastic lesions of the lung surfaces were carefully counted under a microscope, following the method described previously.[14] At the same time, the lungs were perfused with PBS, and a lobe of the left lung was collected and fixed in 10% neutral buffered formalin for histopathological examination. After the experiment, the remaining lungs were stored at −80°C for further study.

Western blot analysis

Thirty micrograms of protein was separated by SDS-PAGE gel and transferred to nitrocellulose membranes and blocked for 1 hour in Tween 20 in Tris-buffered saline (TTBS) containing 5% skim milk. Immunoblotting was carried out by incubating the membranes overnight with corresponding primary antibodies in 5% skim milk at 4°C. The nitrocellulose membrane was then incubated with secondary antibodies conjugated to horseradish peroxidase for 3 hours at room temperature or overnight at 4°C. After washing, the bands were detected by a luminescent image analyzer (LAS-3000; Fujifilm, Tokyo, Japan). Quantification of Western blot bands analysis was performed by Multi Gauge software (version 2.02; Fujifilm).

Histopathological analysis

Lung tissues were fixed in 10% neutral buffered formalin, paraffin-embedded, and sectioned (4 μm). For histological analysis, tissue sections were stained with hematoxylin and eosin (H&E). For immunohistochemistry (IHC), tissue sections were deparaffinized in xylene and rehydrated in serial alcohol gradients 100% to 50% each for 2 minutes. Subsequently, to quench endogenous peroxidase activity, slides were washed and incubated in 3% hydrogen peroxide (AppliChem, Darmstadt, Germany) for 20 minutes. After washing with a TTBS solution, tissue slides were incubated with 3% bovine serum albumin (BSA) in TTBS for 1 hour at room temperature to block the unspecific binding sites. Primary antibodies (dilution of 1:100 in 3% BSA) were applied on tissue sections at 4°C overnight. Tissue slides were washed and incubated in 3% BSA with secondary horseradish peroxide (HRP)-conjugated antibodies (Invitrogen) (dilution of 1:50 in 3% BSA) for 3 hours at room temperature. After washing, the slides were reacted with 3,3′-diaminobenzidine (DAB) (Biosesang, Sungnam, Korea) with constant observation under a light microscope and washed with distilled water.

Tissue slides were counterstained with hematoxylin (DAKO, Carpinteria, CA) and incubated with xylene. Tissue sections were mounted using cover slips and Permount (Fisher Scientific, Waltham, MA) and the slides were reviewed using a light microscope (Carl Zeiss, Thornwood, NY). Quantification of staining intensity of PCNA, VEGF, and CD31 was performed using InStudio software (version 3.01; Pixera, San Jose, CA). In randomly selected fields viewed with appropriate magnification of objective lens, staining intensity was assessed by counting the number of positive cells.

Statistical analysis

Data are expressed as mean values ± standard error of four experiments. Statistical significances were analyzed using Student's *t*-test with two populations in Microcal Origin software (Microcal Software, Northampton, MA). $P < 0.05$ was considered statistically significant, $P < 0.01$ was highly significant, and $P < 0.001$ was more significant when compared with corresponding values. Quantification of Western blot analysis was performed using MultiGauge software (version 2.02; Fujifilm, Tokyo, Japan).

Results

Synthesis and characterization of GT–SPE polyspermine

The GT–SPE was synthesized by the Michael addition reaction between GT and SPE (Figure 1). The composition of the complex was confirmed by ^{1}H NMR (Supplementary Figure 1A). The result of GPC multiangle laser light scattering (GPC-MALS) analysis showed that the molecular weight of GT–SPE was 4.63 kDa with 1.22 polydispersity index (PDI) (Supplementary Figure 1B).

Characterization of GT–SPE/DNA complexes

We confirmed the condensation capability of GT–SPE polyspermine with DNA complex by agarose gel electrophoresis. GT–SPE/DNA complexes were prepared at various weight ratios (0.1–10) by mixing polymer solution with plasmid DNA. The migration of GT–SPE/DNA complex started to be retarded at the weight ratio of 0.5 and was completely retarded at the weight ratio of 5 (Supplementary Figure 2A). As shown in Supplementary Figure 2B, DNA in the GT–SPE complexes was protected from DNase I, however, naked plasmid DNA was degraded. GT–SPE/DNA complexes had a compact and spherical structure (Supplementary Figure 2C). The complexes were formed around 121 nm (PDI: 2.895e-001) and showed relative homogenous size distribution as measured by dynamic light scattering (Supplementary Figure 2D). The zeta potentials of the GT–SPE/DNA complexes were positively charged [+23.45 mV, Mobility: 1.771e-004 (cm2/Vs)] (Supplementary Figure 2E).

Cytotoxicity of GT–SPE

The GT–SPE copolymer showed low cytotoxicity in four different cell lines when compared to PEI 25K (Supplementary Figure 3A–D). GT–SPE copolymer-treated cells showed higher cell viability in A549, HepG2, MCF7, and 16HBE14o- cell lines than PEI 25K-treated cells.

In vitro transfection studies of GT–SPE polyspermine

GT–SPE/DNA showed higher transfection efficiency than naked DNA in luciferase reporter gene expression assay. However, GT–SPE/DNA showed slightly lower transfection efficiency than PEI 25K (Supplementary Figure 4A).

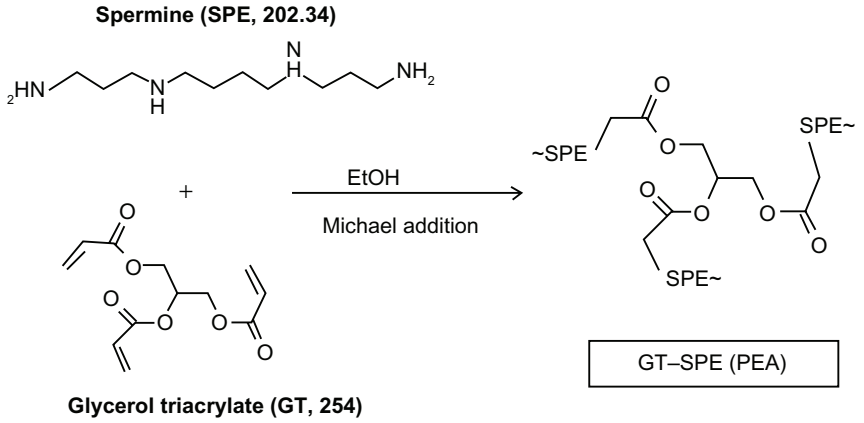

Figure 1 Synthetic scheme of GT–SPE polyspermine.
Abbreviations: GT, glycerol triacrylate; SPE, spermine; PEA, .

To further explain the mechanism of transfection, we analyzed the buffering capacity of GT–SPE copolymer. A549 cells were treated with bafilomycin A1, which is an endosome proton pump inhibitor. In the presence of bafilomycin A1, GT–SPE/DNA complexes showed decreased reporter gene expression levels (Supplementary Figure 4B), likewise for PEI 25K. This suggests that the GT–SPE-mediated gene transfection was due to a proton sponge effect.

In vivo aerosol delivery studies

Based on in vitro increased cellular uptake, high transfection efficiency, and low cytotoxicity data, we performed a GT–SPE gene delivery efficiency test in vivo. The GT–SPE/GFP complex showed much higher fluorescence intensity compared to the control- and naked GFP-treated groups (Figure 2A). In H&E staining, no toxicity was observed in the lungs of the GT–SPE/GFP group (Figure 2B). Moreover, after aerosol delivery, the GFP expression in the lung was dominant compared to other organs (Supplementary Figure 5). In addition, there was no observed lesion in other tissues in H&E staining (Supplementary Figure 6).

Aerosol delivery of Akt1 shRNA with GT–SPE suppressed tumorigenesis

Based on the GFP expression study, Akt1 shRNA with GT–SPE polyspermine was delivered to K-*ras*^{LA1} lung cancer model mice. Aerosol delivery of Akt1 shRNA/GT–SPE significantly decreased the tumor numbers (Figure 3A). The apparent antitumor effects of GT–SPE/Akt1 shRNA are summarized as a graph for better understanding (Figure 3B and C). Lung tumor size in GT–SPE/shAkt-delivered mice was significantly decreased (n = 4, $P < 0.01$ compared to control, shAkt only, and GT–SPE/Scr) and the numbers of tumors measuring over 1 mm tumor were also decreased (n = 4, $P < 0.05$ compared to control; $P < 0.01$ compared to shAkt only; $P < 0.001$ compared to GT–SPE/Scr). Using H&E staining, we also confirmed the tumor suppression effect of GT–SPE/shAkt1 (Figure 3D).

Akt1 shRNA with GT–SPE delivery induced apoptosis and cell cycle arrest and suppressed proliferation

Our results showed that aerosol delivery of GT–SPE/shAkt1 significantly decreased Akt1 expression level (n = 4,

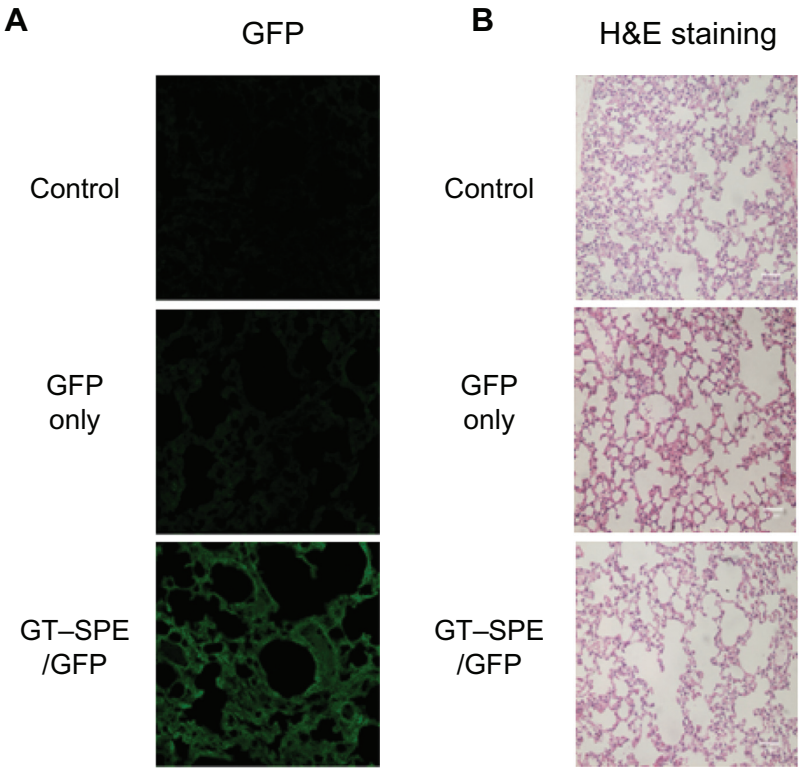

Figure 2 In vivo gene transfer analysis after aerosol delivery to lungs. (**A**) Transfection efficiency study: GFP expression analysis (Magnification, 200×). (**B**) Lung histopathology study: H&E staining (Magnification, 200× ; scale bar, 50 μm).
Abbreviations: GFP, green fluorescent protein; GT–SPE, glycerol triacrylate–spermine; H&E, hematoxylin and eosin.

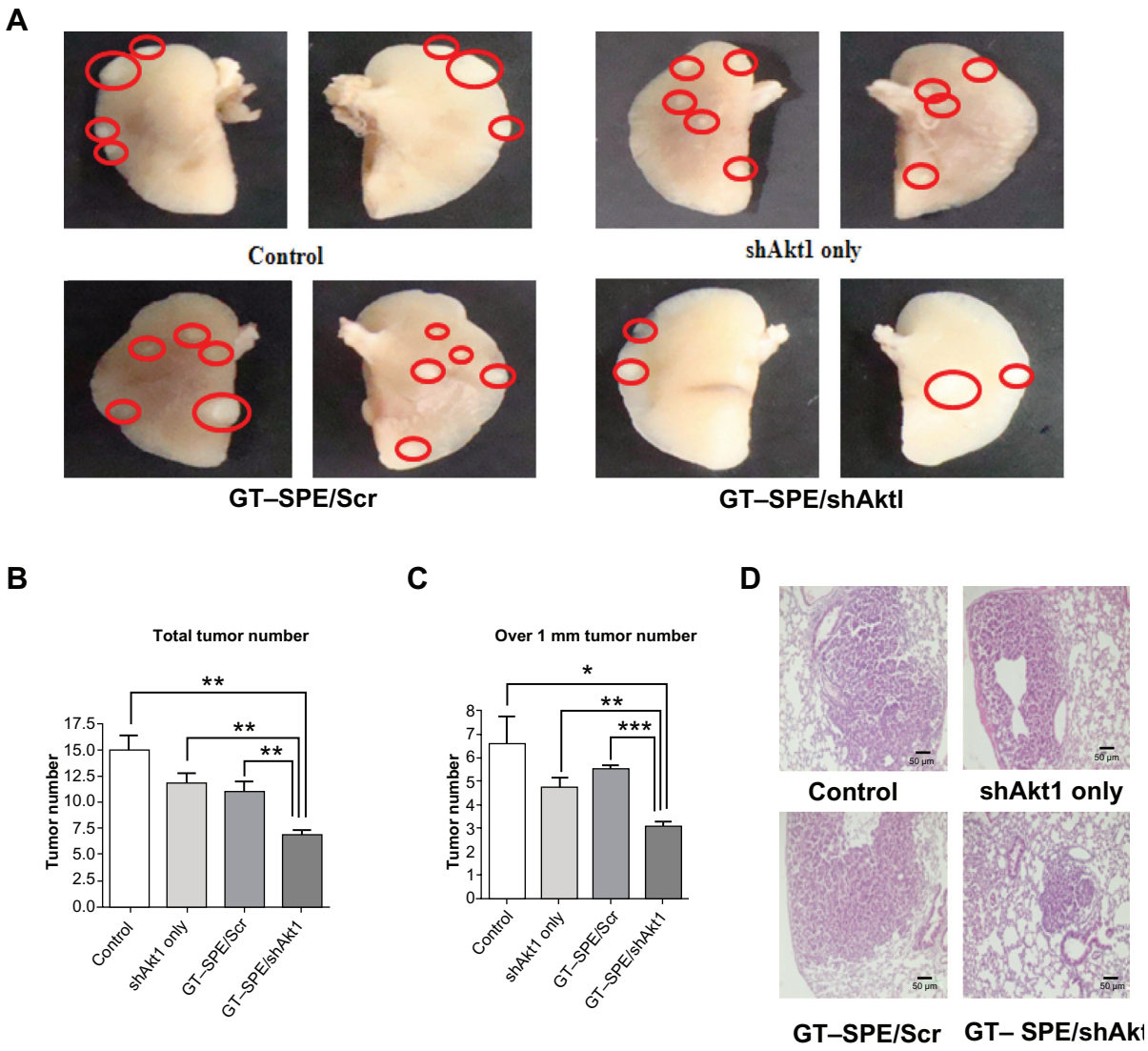

Figure 3 Therapeutic efficiency of GT–SPE as an aerosol gene delivery carrier in lung cancer model K-*ras*^{LA1} mice. Aerosol delivery of GT–SPE/Akt1 shRNA significantly inhibited lung tumor numbers and tumorigenesis. (**A**) Lung tumor lesions. (**B**) Total tumor numbers (n = 4, $^{**}P < 0.01$ compared to shAkt1 only, GT–SPE/Scr, and control). (**C**) Tumor size over 1 mm; tumor numbers (n = 4, $^{*}P < 0.05$ compared to control; $^{**}P < 0.01$ compared to shAkt1 only; $^{***}P < 0.001$ compared to GT–SPE/Scr). (**D**) Histopathological features (Magnification, 200×).

Abbreviations: GT–SPE, glycerol triacrylate–spermine; MMP-9, matrix metalloprotease-9; PCNA, proliferating cell nuclear antigen; shAkt1, small hairpin Akt1.

$P < 0.01$ compared to control; $P < 0.05$ compared to shAkt1 only and GT–SPE/Scr). To determine whether repeated aerosol-delivered GT–SPE/shAkt1 might induce apoptosis, the expressions of Bcl-xL (one of the antiapoptotic proteins) and Bax (a proapoptotic protein) proteins were examined. There was a significant decrease in the expression level of Bcl-xL in the GT–SPE/shAkt1-delivered group (n = 4, $P < 0.01$ compared to control, shAkt1 only, and GT–SPE/shAkt1). In contrast, there was a significant increase in the expression level of Bax in the GT–SPE/shAkt1 inhalation group (n = 4, $P < 0.01$ compared to control and GT–SPE/Scr; $P < 0.001$ compared to shAkt1 only) (Figure 4A–D). In addition, to examine whether aerosol-delivered GT–SPE/shAkt1 also inhibits the cell cycle, we performed a Western blot analysis and observed that the level of cyclin B1 protein was significantly decreased in the treated group (Figure 5A), as confirmed by densitometric analysis (n = 4, $P < 0.01$ compared to control, shAkt1 only, and GT–SPE/Scr) (Figure 5B). To analyze the degree of cell proliferation in tumor tissue, Western blot and IHC analyses were performed. In the GT–SPE/shAkt1-delivered group, the expression level of PCNA was significantly decreased (Figure 5A) and it was further confirmed by densitometric analysis (n = 4, $P < 0.01$ compared to control and GT–SPE/Scr; $P < 0.05$ compared to shAkt1 only) (Figure 5C). IHC data further confirmed that delivery of GT–SPE/shAkt1 suppressed the expression of PCNA in the lung tumor tissue (Figure 5D).

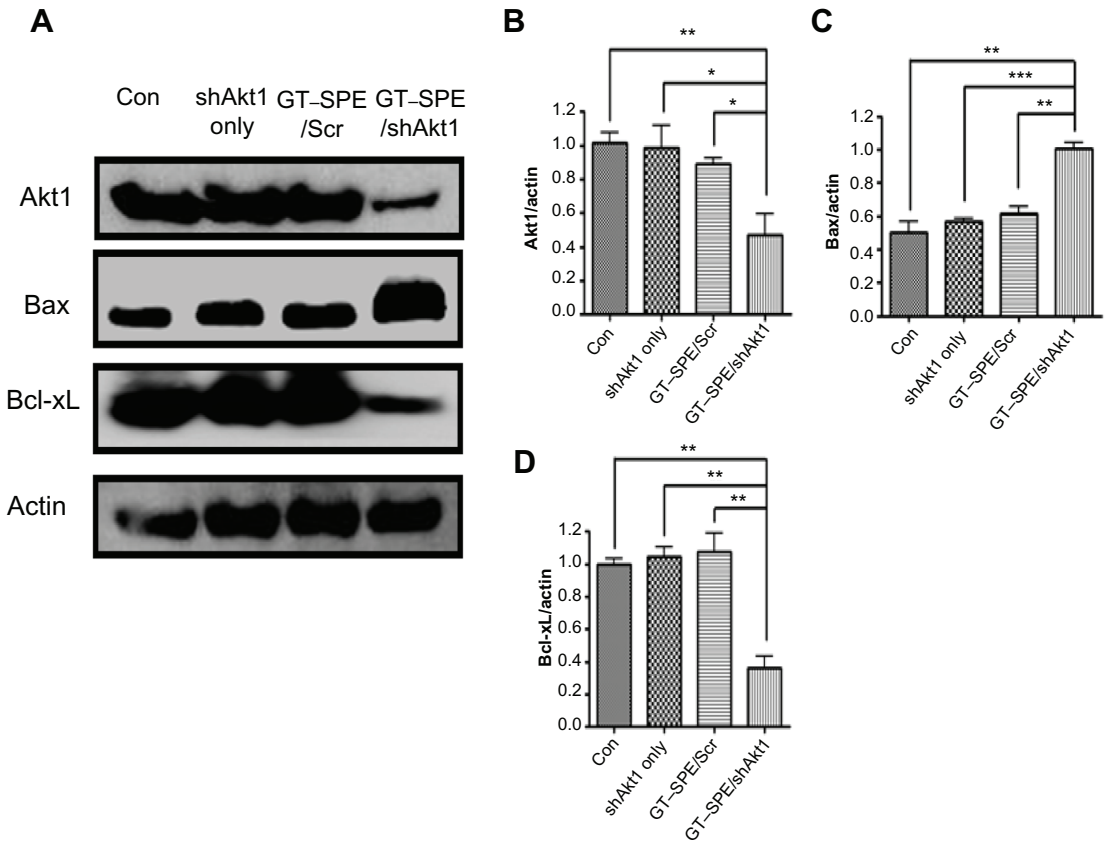

Figure 4 shAkt1 aerosol delivery significantly decreased Akt1 expression level and induced apoptosis. (**A**) Western blot bands. Statistical analyses of Western blot (**B**) Akt1, (**C**) Bax, and (**D**) Bcl-xL. Bands were analyzed by densitometer (n = 4, $*P < 0.05$, $**P < 0.01$, and $***P < 0.001$ compared to shAkt1 only, GT–SPE/Scr, and control).
Abbreviations: con, control; GT–SPE, glycerol triacrylate–spermine; shAkt1, small hairpin Akt1.

Inhibited angiogenesis, tumor vessel density, and decreased MMP-9 activity were evident in Akt1 shRNA with GT–SPE-delivered group

MMP-9 was examined for the analysis of invasion and metastasis of cancer via the destruction of the extracellular matrix and membrane. The expression levels of MMP-9 were significantly decreased in the GT–SPE/shAkt1-delivered group (Figure 6A) and confirmed by densitometric analysis (n = 4, $P < 0.05$ compared to control; $P < 0.01$ compared to shAkt1 only and GT–SPE/Scr) (Figure 6B). For the analysis of tumorigenesis, VEGF, which is an important marker for tumor progression, was analyzed using Western blot and IHC. Our data revealed that the expression levels of VEGF were significantly decreased in the GT–SPE/shAkt1-treated group (Figure 6A and E) and the results were analyzed using densitometric analysis (n = 4, $P < 0.01$ compared to control and GT–SPE/Scr; $P < 0.001$ compared to shAkt1 only) (Figure 6C). To examine tumor vascular density, the CD31 expression level was analyzed. Our results clearly showed decreased expression of CD31 in the shAkt1-delivered group as determined by Western blot and IHC analyses (n = 4, $P < 0.01$ compared to control, shAkt1 only, and GT–SPE/Scr) (Figure 6D and E).

Discussion

SPE is a tetraamine with two primary and two secondary amino groups that are involved in cellular metabolism.[15,16] SPE is a safe endogenous molecule found in all eukaryotic cells, but it has low molecular weight and less amine density. To overcome this problem, we synthesized polyspermine using the Michael addition reaction between acrylate groups of GT and amine groups of SPE (Figure 1). The polymerization of SPE with GT to form GT–SPE was confirmed by ^{1}H NMR and GPC analysis. In ^{1}H NMR spectrum, the peaks for spermine proton ($–CH_2–CH_2–$, $\delta = 1.6–1.8$ ppm) and peaks for GT proton ($–CH_2–$, $\delta = 3.8$ ppm) were clearly visible, indicating successful coupling of SPE molecule with GT (Supplementary Figure 1A).

To confirm the condensation capability of GT–SPE, we performed gel electrophoresis assay over various weight ratios (0.1–10) of GT–SPE/DNA complexes. At the weight

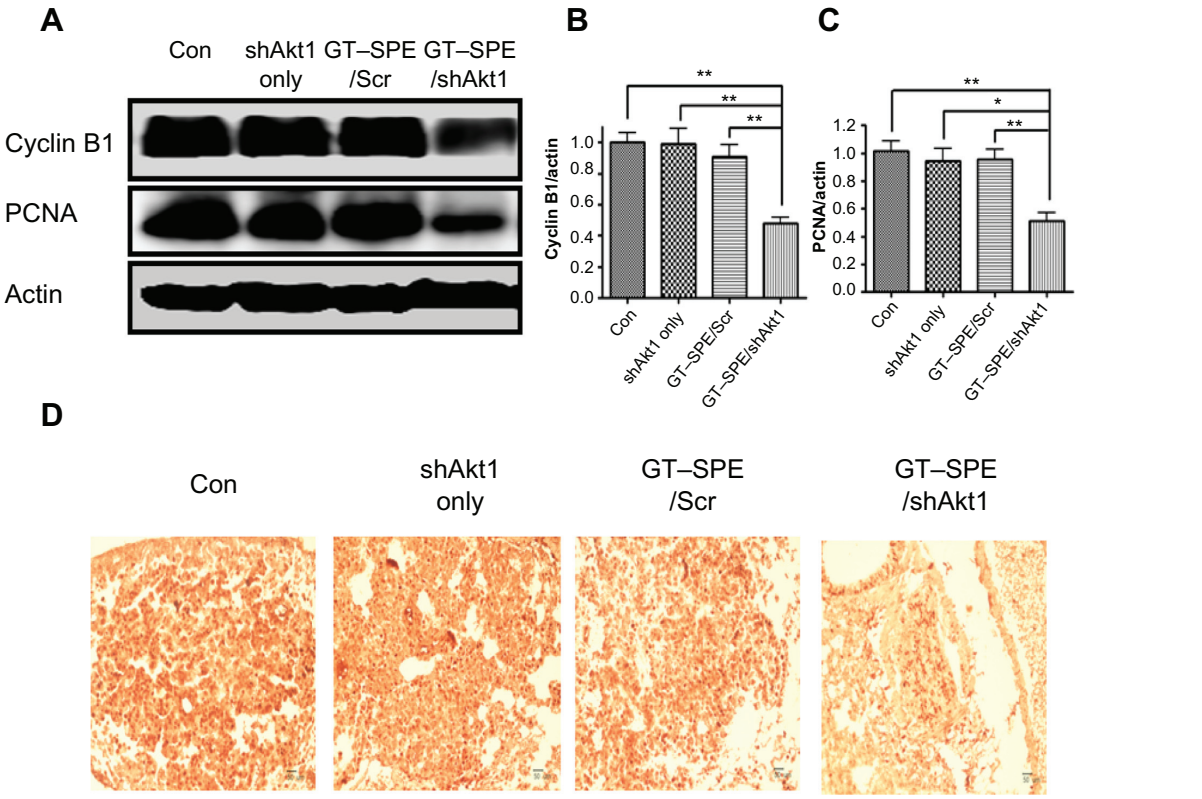

Figure 5 GT–SPE/shAkt1 induced cell cycle arrest and inhibited proliferation. (**A**) Western blot bands of Cyclin B1 and PCNA, (**B**) Cyclin B1, and (**C**) PCNA. Bands were analyzed by densitometer (n = 4, $*P < 0.05$, $**P < 0.01$, and $***P < 0.001$ compared to shAkt1 only, GT–SPE/Scr and control). (**D**) PCNA immunohistochemistry analysis (Magnification, 200×; scale bar, 50 μm).

Abbreviations: con, control; GT–SPE, glycerol triacrylate–spermine; PCNA, proliferating cell nuclear antigen; shAkt1, small hairpin Akt1.

ratio of 0.5, initiation of copolymer retardation and DNA complex occurred and, at the weight ratio of 5, the migration of complexes was totally inhibited (Supplementary Figure 2A), suggesting that GT–SPE polyspermine was completely bound to the DNA. Thus, a GT–SPE/DNA weight ratio of 5 was determined for the rest of the study. Surface charge measurement indicated that GT–SPE complexes were +23.45 mV in ζ-potential at 5:1 (GT–SPE/DNA) ratio (Supplementary Figure 2E). A positive charged surface is necessary for binding to a negatively charged cell membrane.[17,19] Consequently, all of these features suggest that the newly synthesized GT–SPE carrier is adequate for gene delivery.

As high-molecular-weight PEI (25 kDa) is one of the most potent polymeric vectors because of its high pH-buffering capacity of endosomal escape, we compared the cytotoxicity and transfection efficiency of GT–SPE with PEI 25K. GT–SPE showed lower cytotoxicity than PEI 25K in four different cell lines: A549, HepG2, MCF7, and 16HBE14o- (Supplementary Figure 3A–D). Toxicologically, cationic nanoparticles (NPs) are more toxic than their anionic counterparts.[20] In addition, there is a different report that states that both positively and negatively charged NPs are toxic, with the negative NPs evoking a greater response.[21] PEI 25K polyplex used in this study showed ζ-potential of +39.17 mV in N/P ratio of 10 and GT–SPE/DNA polyplex displayed lower ζ-potential (+23.45 mV) at a weight ratio of 5. Although the mechanism of PEI toxicity is poorly understood, this surface charge difference can be one of the main reasons for the lower toxicity of GT–SPE. Aggregation of PEI on the cell surface, as well as damage of cell membrane function, may be another reason of PEI toxicity, because PEI 25K lacks degradable linkages. On the other hand, GT–SPE polyspermine has biodegradable ester bond linkages and spermine is a biogenic tetraamine, which is safe and naturally present in eukaryotic cells. Even though GT–SPE showed slightly lower transfection efficiency than PEI 25K (Supplementary Figure 4A), it showed significantly effective transfection capability (higher than 10^5 RLU/mg protein). High transfection efficiency of PEI 25K is believed to originate from the so-called intrinsic "proton sponge" effect in which partially protonated PEI brings in more protons inside the endocytic vesicles embedded with ATPase proton pumps. It is accompanied by an influx of chloride counter-ions, finally rupturing

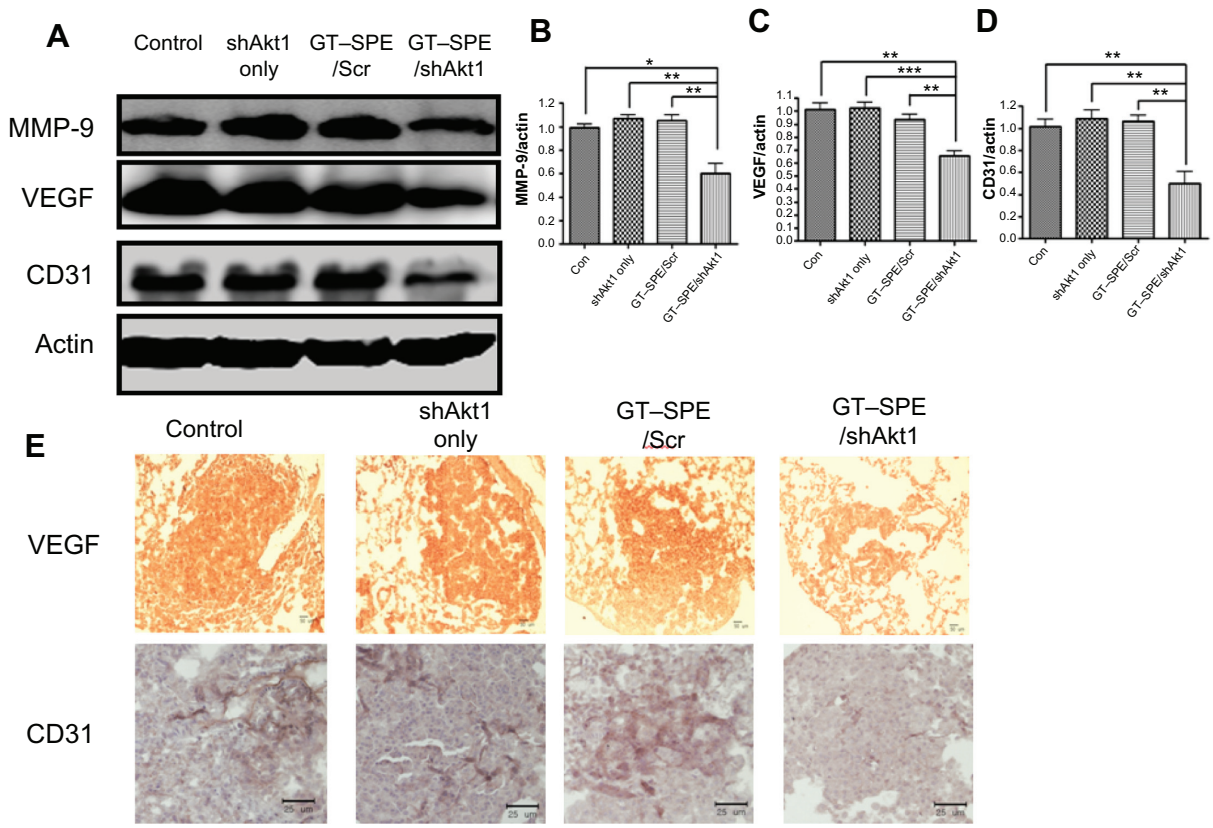

Figure 6 Repeated aerosol delivery of GT–SPE/shAkt1 decreased MMP-9 activity and angiogenesis. (**A**) Western blot bands of MMP-9, VEGF, and CD31. (**B**) MMP-9, (**C**) VEGF, (**D**) CD31. Bands were analyzed by densitometer (n = 4, $*P < 0.05$, $**P < 0.01$, and $***P < 0.001$ compared to shAkt1 only, GT–SPE/Scr, and control). (**E**) VEGF and CD31 immunohistochemistry (Magnification, 200×; scale bar, 50 μm).
Abbreviations: GT–SPE, glycerol triacrylate–spermine; MMP-9, matrix metalloprotease-9; shAkt1, small hairpin Akt1; VEGF, vascular endothelial growth factor.

endocytic vesicles due to higher osmotic pressure.[22] Because every third atom of PEI is nitrogen, it has a very high density of amines, only 15%–20% of which are protonated at physiological pH.[23] This unique property makes PEI an extraordinarily strong proton sponge.[24] In order to determine whether the transfection mechanism of GT–SPE is similar to PEI 25K, we used bafilomycin A1 as an inhibitor of endosomal ATPase proton pump.[25] When GT–SPE/DNA complex was treated with bafilomycin A1, there was a large decrease in the transfection efficiency of the complex, as demonstrated in PEI 25K (Supplementary Figure 4B). Though SPE itself has less amine density, GT–SPE polyspermine acquired enough buffering capacity for efficient gene delivery by polymerizing of SPE using GT. Therefore, our results suggest that GT–SPE polyspermine can be used as a safe and efficient biocompatible gene delivery carrier.

Unlike in vitro gene delivery, requisites for successful in vivo gene delivery carrier are much more complex. Among the various routes for drug delivery, pulmonary delivery provides much faster absorption of small molecules, with much less metabolism. Furthermore, lung tissue is naturally permeable and functions as a non-invasive port for the entry of substances into the circulatory system.[26] To test the possibility of inhalation gene therapy of a newly synthesized carrier, we first checked the GFP gene transfection efficiency of GT–SPE. We delivered GT–SPE/GFP complexes to mice and observed fluorescence expressions in the lungs under confocal laser scanning microscope (CLSM). The results revealed that the GFP signal of GT–SPE/GFP was more dominant in the lungs of the treated group than the control and the naked GFP groups (Figure 2A and Supplementary Figure 5). In H&E staining, no lesion was observed in the lung tissues of the GT–SPE/GFP group when compared to the control (Figure 2B and Supplementary Figure 6). These data propose the potential application of GT–SPE in inhalation gene therapy as an efficient and safe carrier system.

We also tested the therapeutic efficacy of repeated aerosol delivery of therapeutic gene to the lung cancer mouse model, because repeated gene delivery may cause toxicity with incomplete efficacy.[27] Furthermore, the majority of airway epithelial cells are slowly dividing or terminally differentiated, thus, necessitating the test of repeated administration

of gene transfer vectors for long transgenic expression.[28] We targeted Akt1 as a gene to be downregulated because about 90% of NSCLC is associated with constitutive activation of Akt pathway.[29] Furthermore, a previous study has shown that aerosol delivery of shAkt1 with polymer carrier can suppress the tumorigenesis.[3] In this regard, we delivered GT–SPE/shAkt1 complexes to the lung of the K-*ras*^{LA1} lung cancer mouse model. Akt pathway regulates Bcl-2 family members and apoptotic activity,[30] thus, inhibition of Akt1 with GT–SPE by repeated aerosol shAkt1 deliveries may facilitate apoptosis. The expression level of proapoptotic protein Bax was significantly increased, whereas expression level of antiapoptotic protein Bcl-xL was significantly decreased in shAkt1 with GT–SPE repeated delivery group when compared to the other groups (Figure 4). These results showed that GT–SPE/shAkt1 successfully suppressed tumorigenesis through the blockage of Akt signaling pathways and induced apoptosis, which was confirmed by total tumor numbers, histopathology, and Western blot data (Figures 3 and 4).

The degrees of cell cycle protein and proliferation were examined with respect to tumor progression. In higher eukaryotes, cyclin B1 and A2 are required for the completion of the G2/M transition phase.[31] In cancers, mutations of proteins that regulate progression are frequent; it can lead to abnormal cell cycle transition control.[32] Our data revealed that expression levels of cyclin B1 were significantly decreased in the treated group (Figure 5A and B). This means that repeatedly delivered GT–SPE/shAkt1 played an important role in cell cycle inhibition and it showed similar changes with respect to Akt1 expression level (Figures 4A and 5A). Phosphatidyl inositol 3-kinase (PI3K)/Akt pathway has a critical impact on cell growth, proliferation, and regulation of the cell cycle.[33] PCNA is a cell nucleus antigen that is expressed during DNA synthesis.[34] Aerosol-delivered GT–SPE/shAkt1 significantly decreased the expression level of PCNA in lung tumor tissues, which was confirmed by Western blot and IHC (Figure 5A–D). In lung tumor tissues, cell proliferations were also suppressed in the treated group by repeated and efficient shAkt1 deliveries.

MMPs functions in basal membrane and extracellular matrix destructions and are associated with the metastasis of tumors.[35] In addition, MMP-9 expression is highly related to metastasis in lung, liver, and breast carcinomas.[36] For these reasons, MMP-9 expression levels were examined by Western blot. Our data showed significantly decreased expression levels of MMP-9 in the GT–SPE/shAkt1 repeated delivery group. VEGF is an essential cytokine associated with stimulating endothelial cell growth and angiogenesis.[37] The expression levels of VEGF were also examined using Western blot and IHC. CD31 is an endothelial antigen and vasculature marker and it can be used to determine the density of intratumoral vessels and the degree of neoangiogenesis.[38] Significantly lower expression levels of VEGF and CD31 were revealed by Western blot analysis and low intensities at IHC in the repeated delivery group (Figure 6A–D). It was concluded that decreased expression of MMP-9, VEGF, and CD31 in the GT–SPE/shAkt1-delivered group showed significant inhibition of metastasis through repeated inhalation treatments. The result of this study may only show preliminary characteristics because obtained data were based on a limited number of animals (four per group), therefore, future experiments are necessary to clarify the efficiency of GT–SPE for gene delivery. These studies are currently underway.

Conclusion

In this study, we have described the successful preparation of a novel polyspermine, GT–SPE polymer, and evaluated the possibility of its use as a new gene carrier for lung cancer gene therapy. The GT–SPE copolymer showed a significant ability to form complexes with DNA and possessed suitable physicochemical properties as a gene delivery carrier system. This copolymer had low cytotoxicity and showed enhanced gene transfer efficiency both in vitro and in vivo. Aerosol delivery of GT–SPE/shAkt1 significantly suppressed lung tumorigenesis through apoptosis with no organ toxicity. Therefore, GT–SPE has the potential to serve as a biocompatible and efficient aerosol gene carrier system.

Acknowledgments

This work was partly supported by the R&D Program of MKE/KEIT (10035333, Development of anticancer therapeutic agent based on regulating cell cycle or cell death), as well as by the National Research Foundation (NRF-2011-0000380 and NRF-2011-0002169) and the Ministry of Education, Science and Technology (MEST) in Korea. MHC was also partially supported by the Research Institute for Veterinary Science, Seoul National University.

Disclosure

The authors report no conflicts of interest in this work.

References

1. McManus MT, Sharp PA. Gene silencing in mammals by small interfering RNAs. *Nat Rev Genet*. 2002;3(10):737–747.
2. Kim SH, Mok H, Jeong JH, et al. Comparative evaluation of target-specific GFP gene silencing efficiencies for antisense ODN, synthetic siRNA, and siRNA plasmid complexed with PEI-PEG-FOL conjugate. *Bioconjug Chem*. 2006;17(1):241–244.

3. Jiang HL, Xu CX, Kim YK, et al. The suppression of lung tumorigenesis by aerosol-delivered folate-chitosan-graft-polyethylenimine/Akt1 shRNA complexes through the Akt signaling pathway. *Biomaterials*. 2009;30(29):5844–5852.
4. Aagaard L, Rossi JJ. RNAi therapeutics: principles, prospects and challenges. *Adv Drug Deliv Rev*. 2007;59(2–3):75–86.
5. Kim WJ, Kim SW. Efficient siRNA delivery with non-viral polymeric vehicles. *Pharm Res*. 2009;26(3):657–666.
6. Luo D, Saltzman WM. Synthetic DNA delivery systems. *Nat Biotechnol*. 2000;18(1):33–37.
7. Elsabahy M, Nazarali A, Foldvari M. Non-viral nucleic acid delivery: key challenges and future directions. *Curr Drug Deliv*. 2011;8(3):235–244.
8. Mohammadi Z, Abolhassani M, Dorkoosh FA, et al. Preparation and evaluation of chitosan-DNA-FAP-B nanoparticles as a novel non-viral vector for gene delivery to the lung epithelial cells. *Int J Pharm*. 2011;409(1–2):307–313.
9. Lungwitz U, Breunig M, Blunk T, Gopferich A. Polyethylenimine-based non-viral gene delivery systems. *Eur J Pharm Biopharm*. 2005;60(2):247–266.
10. Boussif O, Lezoualc'h F, Zanta MA, Mergny MD, Scherman D, Demeneix B. A versatile vector for gene and oligonucleotide transfer into cells in culture and in vivo: polyethylenimine. *Proc Natl Acad Sci U S A*. 1995;92(16):7297–7301.
11. Beyerle A, Irmler M, Beckers J, Kissel T, Stoeger T. Toxicity pathway focused gene expression profiling of PEI-based polymers for pulmonary applications. *Mol Pharm*. 2010;7(3):727–737.
12. Choi YJ, Kang SJ, Kim YJ, Lim YB, Chung HW. Comparative studies on the genotoxicity and cytotoxicity of polymeric gene carriers polyethylenimine (PEI) and polyamidoamine (PAMAM) dendrimer in Jurkat T-cells. *Drug Chem Toxicol*. 2010;33(4):357–366.
13. Jiang HL, Kim YK, Arote R, Nah JW, Cho MH, Choi YJ, et al. Chitosan-graft-polyethylenimine as a gene carrier. *J Control Release*. 2007;117(2):273–280.
14. Singh RP, Deep G, Chittezhath M, et al. Effect of silibinin on the growth and progression of primary lung tumors in mice. *J Natl Cancer Inst*. 2006;98(12):846–855.
15. Jiang HL, Lim HT, Kim YK, et al. Chitosan-graft-spermine as a gene carrier in vitro and in vivo. *Eur J Pharm Biopharm*. 2011;77(1):36–42.
16. Allen JC. Biochemistry of the polyamines. *Cell Biochem Funct*. 1983;1(3):131–140.
17. Kunath K, von Harpe A, Fischer D, et al. Low-molecular-weight polyethylenimine as a non-viral vector for DNA delivery: comparison of physicochemical properties, transfection efficiency and in vivo distribution with high-molecular-weight polyethylenimine. *J Control Release*. 2003;89(1):113–125.
18. Jiang HL, Kwon JT, Kim EM, et al. Galactosylated poly(ethylene glycol)-chitosan-graft-polyethylenimine as a gene carrier for hepatocyte-targeting. *J Control Release*. 2008;131(2):150–157.
19. Jiang HL, Kwon JT, Kim YK, et al. Galactosylated chitosan-graft-polyethylenimine as a gene carrier for hepatocyte targeting. *Gene Ther*. 2007;14(19):1389–1398.
20. Goodman CM, McCusker CD, Yilmaz T, Rotello VM. Toxicity of gold nanoparticles functionalized with cationic and anionic side chains. *Bioconjug Chem*. 2004;15(4):897–900.
21. Schaeublin NM, Braydich-Stolle LK, Schrand AM, et al. Surface charge of gold nanoparticles mediates mechanism of toxicity. *Nanoscale*. 2011;3(2):410–420.
22. Behr JP. The proton sponge: a trick to enter cells the viruses did not exploit. *Chimia*. 1997;51(1–2):34–36.
23. Suh J, Paik HJ, Hwang BK. Ionization of poly (ethylenimine) and poly (allylamine) at various pH's. *Bioorg Chem*. 1994;22(3):318–327.
24. Pack DW, Hoffman AS, Pun S, Stayton PS. Design and development of polymers for gene delivery. *Nat Rev Drug Discov*. 2005;4(7):581–593.
25. Kichler A, Leborgne C, Coeytaux E, Danos O. Polyethylenimine-mediated gene delivery: a mechanistic study. *J Gene Med*. 2001;3(2):135–144.
26. Patton JS, Byron PR. Inhaling medicines: delivering drugs to the body through the lungs. *Nat Rev Drug Discov*. 2007;6(1):67–74.
27. Ferrari S, Griesenbach U, Geddes DM, Alton E. Immunological hurdles to lung gene therapy. *Clin Exp Immunol*. 2003;132(1):1–8.
28. Zhou HS, Liu DP, Liang CC. Challenges and strategies: the immune responses in gene therapy. *Med Res Rev*. 2004;24(6):748–761.
29. David O. Akt and PTEN: new diagnostic markers of non-small cell lung cancer? *J Cell Mol Med*. 2001;5(4):430–433.
30. Yang J, Liu X, Bhalla K, et al. Prevention of apoptosis by Bcl-2: release of cytochrome C from mitochondria blocked. *Science*. 1997;275(5303):1129–1132.
31. Sánchez I, Dynlacht BD. New insights into cyclins, CDKs, and cell cycle control. *Semin Cell Dev Biol*. 2005;16(3):311–321.
32. Molinari M. Cell cycle checkpoints and their inactivation in human cancer. *Cell Prolif*. 2000;33(5):261–274.
33. Dillon RL, White DE, Muller WJ. The phosphatidyl inositol 3-kinase signaling network: implications for human breast cancer. *Oncogene*. 2007;26(9):1338–1345.
34. Leonardi E, Girlando S, Serio G, et al. PCNA and Ki67 expression in breast carcinoma: correlations with clinical and biological variables. *J Clin Pathol*. 1992;45(5):416–419.
35. Jezierska A, Motyl T. Matrix metalloproteinase-2 involvement in breast cancer progression: a mini-review. *Med Sci Monit*. 2009;15(2):RA32–RA40.
36. Curran S, Murray GI. Matrix metalloproteinases in tumour invasion and metastasis. *J Pathol*. 1999;189(3):300–308.
37. Niklińska W, Burzykowski T, Chyczewski L, Niklinski J. Expression of vascular endothelial growth factor (VEGF) in non-small cell lung cancer (NSCLC): association with p53 gene mutation and prognosis. *Lung Cancer*. 2001;34(Suppl 2):S59–S64.
38. Mineo TC, Ambrogi V, Baldi A, et al. Prognostic impact of VEGF, CD31, CD34, and CD105 expression and tumour vessel invasion after radical surgery for IB-IIA non-small cell lung cancer. *J Clin Pathol*. 2004;57(6):591–597.

Supplementary figures

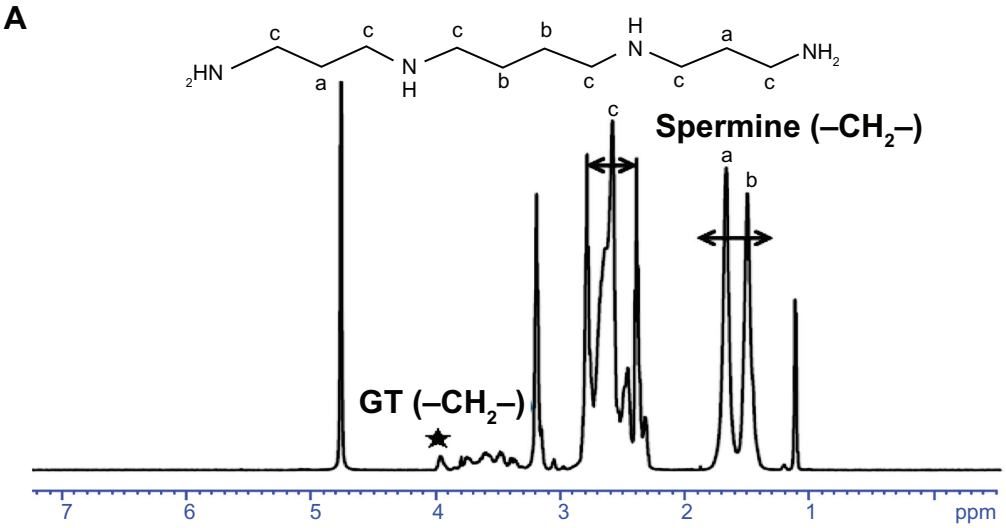

B

GPC analysis

	Mw	Mn	PDI
GT-SPE	4630	3790	1.22

Figure S1 Characterizations of GT–SPE polyspermine. (**A**) ^{1}H NMR spectra of GT–SPE. (**B**) GPC analysis of GT–SPE.
Abbreviations: GPC, gas permeability chromatography; GT–SPE, glycerol triacrylate–spermine; ^{1}H NMR, proton nuclear magnetic resonance; PDI, polydispersity index.

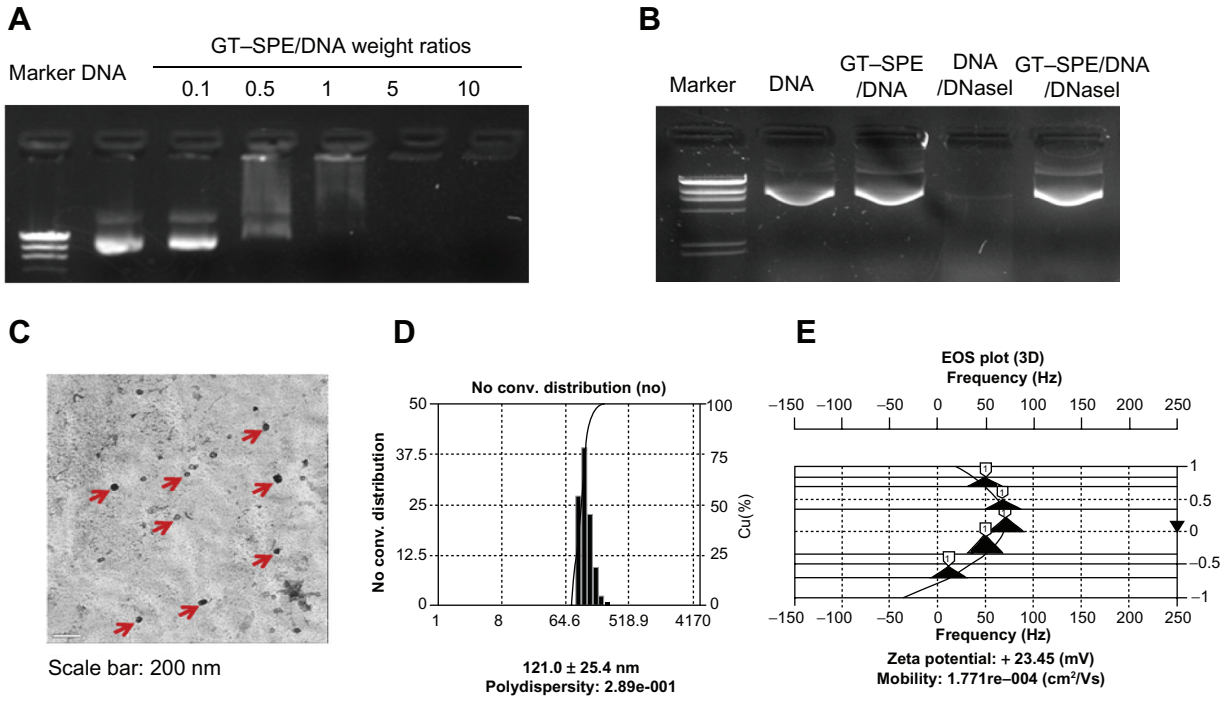

Figure S2 Characterizations of GT–SPE/DNA complexes. (**A**) Agarose gel electrophoresis of GT–SPE/DNA complexes at various weight ratios of the complexes. (**B**) DNA protection and release assay. (**C**) EF-TEM images of GT–SPE/DNA complexes. (**D**) Size distribution assay. (**E**) Particle surface charges of copolymer/DNA complexes.
Abbreviations: EF-TEM, energy-filtered transmission electron microscopy; GT–SPE, glycerol triacrylate–spermine.

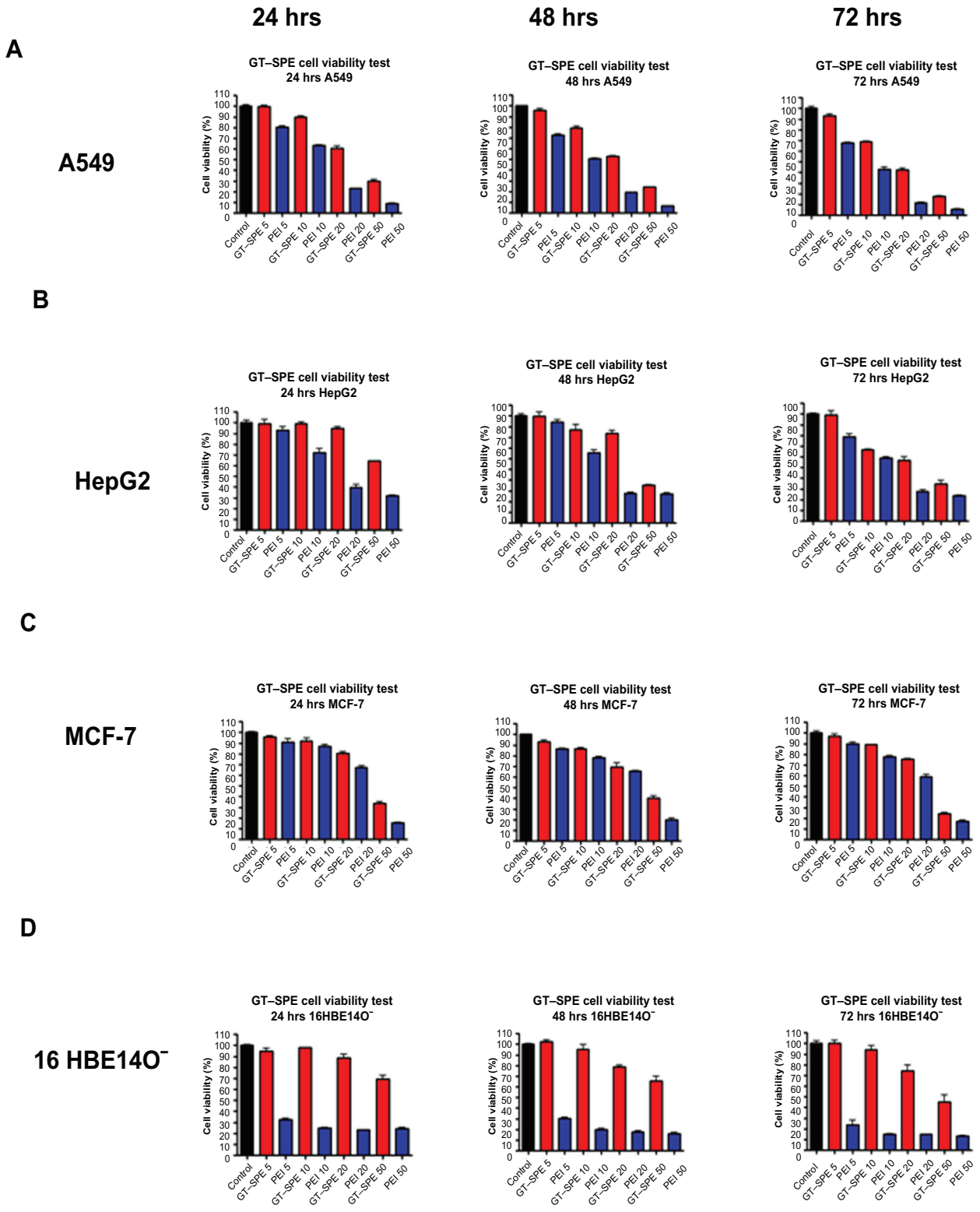

Figure S3 Cytotoxicity of GT–SPE copolymer at various concentrations in different cell lines. (**A**) A549, (**B**) HepG2, (**C**) MCF7, and (**D**) 16HBE14o- (mean ± SD, n = 3).
Abbreviations: GT–SPE, glycerol triacrylate–spermine; PEI, polyethylenimine; SD, standard deviation.

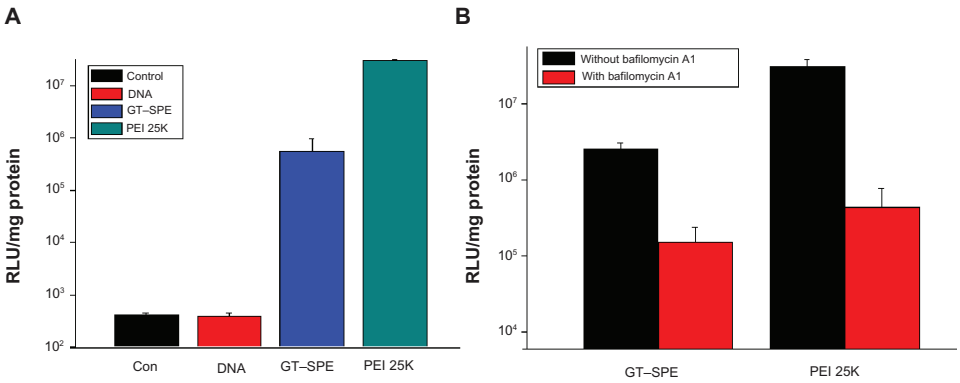

Figure S4 In vitro transfection studies. (**A**) Transfection efficiency study in A549 cells by GT–SPE/DNA (pGL3) complexes at various weight ratios (mean ± SD, n = 3). (**B**) Buffering capacity study of GT–SPE/DNA complexes in A549 cells (mean ± SD, n = 3).
Abbreviations: con, control; GT–SPE, glycerol triacrylate–spermine; PEI, polyethylenimine; SD, standard deviation.

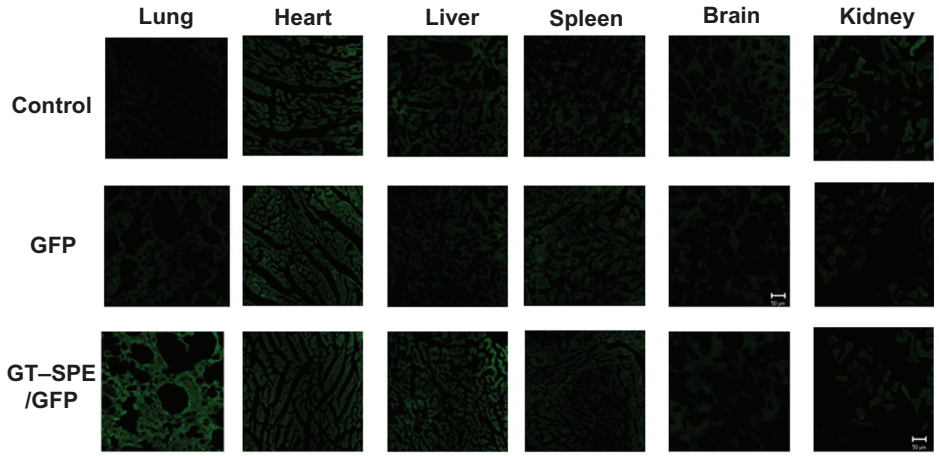

Figure S5 In vivo GFP analysis in different organs after aerosol administration.
Abbreviations: GFP, green fluorescent protein; GT–SPE, glycerol triacrylate–spermine.

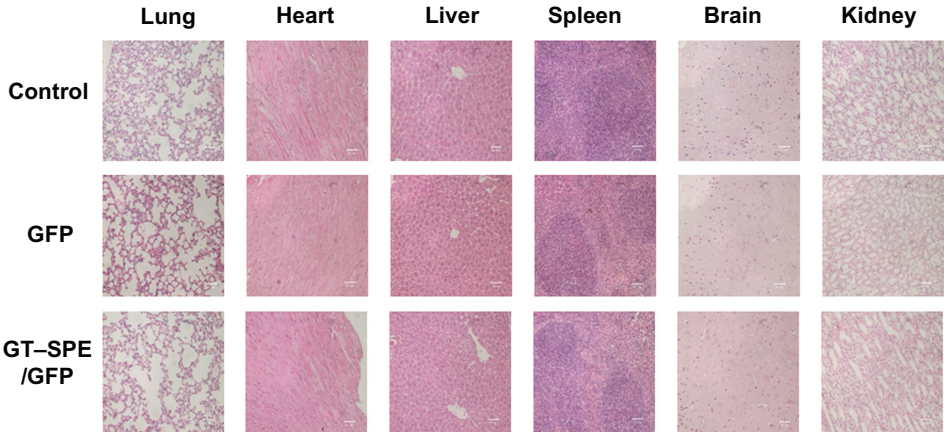

Figure S6 In vivo H&E staining in different organs after aerosol administration (magnification: 200×).
Abbreviations: GFP, green fluorescent protein; GT–SPE, glycerol triacrylate–spermine; H&E, hematoxylin and eosin.